Highly Symmetric Patchy Multicompartment Nanoparticles from the Self-Assembly of ABC Linear Terpolymers in C-Selective Solvents

ARTICLE *in* LANGMUIR · JULY 2012

Impact Factor: 4.46 · DOI: 10.1021/la3014943 · Source: PubMed

4 AUTHORS, INCLUDING:

Yutian Zhu
Chinese Academy of Sciences
43 PUBLICATIONS **355** CITATIONS

SEE PROFILE

Langmuir

Article

pubs.acs.org/Langmuir

Highly Symmetric Patchy Multicompartment Nanoparticles from the Self-Assembly of ABC Linear Terpolymers in *C*-Selective Solvents

Weixin Kong,[†] Wei Jiang,[†] Yutian Zhu,*[,†] and Baohui Li*[,‡]

[†]State Key Laboratory of Polymer Physics and Chemistry, Changchun Institute of Applied Chemistry, Chinese Academy of Sciences, Changchun, 130022, China

[‡]College of Physics and Key Laboratory of Functional Polymer Materials of Ministry of Education, Nankai University, Tianjin, 300071, China

ABSTRACT: Multicompartment micelles, especially those with highly symmetric surfaces such as patchy-like, patchy, and Janus micelles, have tremendous potential as building blocks of hierarchical multifunctional nanomaterials. One of the most versatile and powerful methods to obtain patchy multicompartment micelles is by the solution-state self-assembly of linear triblock copolymers. In this article, we applied the simulated annealing method to study the self-assembly of ABC linear terpolymers in *C*-selective solvents. Simulations predict a variety of patchy and patchy-like multicompartment micelles with high symmetry and also yield a detailed phase diagram to reveal how to control the patchy multicompartment micelle morphologies precisely. The phase diagram demonstrates that the internal segregated micellar structure depends on the ratio between the volume fractions of the two solvophobic blocks and their incompatibility, whereas the overall micellar shape depends on the copolymer concentration. The relationship between the interfacial energy, stretching energy of chains and the micellar morphology, micellar morphological transition are elucidated by computing the average contact number among the species, the mean square end-to-end distances of the whole terpolymers, the AB blocks in the terpolymers, the AB diblock copolymers, and angle distribution of terpolymers. The anchoring effect of the solvophilic *C* block on micellar structures is also examined by comparing the morphologies formed from ABC terpolymers and AB diblock copolymers.

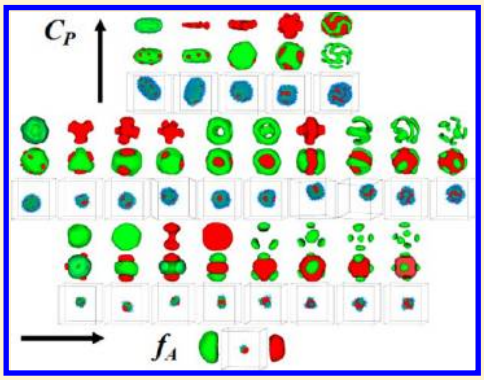

INTRODUCTION

Utilizing the spontaneous self-assembly of building blocks, such as atoms, macromolecules, and nanoparticles, is one of the bottom-up strategies to create hierarchical multifunctional nanomaterials that can be used in many fields.[1] A dramatic example is a living creature, including a variety of species from the simplest (blue-green algae) to the most complex (humans). In abiotic areas, self-assembly is also ubiquitous in different scales. For the past decades, clusters formed from self-assembly of the smallest building blocks, i.e., atoms, attracted great attention due to their novel photonic, electronic, and magnetic properties and geometry that differ from the bulk phase. In the intermediate scale, spontaneous formation of macromolecules in melt and solution has many potential applications such as nanolithography,[2] biomineralization,[3] and drug delivery.[4] In relatively larger scales, nanoparticle self-assembly recently stimulated much interest for its potential applications in studying nucleation and glass transition[5,6] and in producing hierarchical multifunctional materials.

The aforementioned nanoparticles can be classified into two types: one with isotropic surfaces and the other with anisotropic surfaces. Studies on the geometry of clusters consisting of atoms are limited by nonequilibrium conditions, shorter cluster lifetimes, and difficulties in obtaining the structure of individual clusters, although understanding nucleation and glass transition are helpful.[7] Isotropic nanoparticles are so large they can be observed under optical microscopy. However, they are still sufficiently small to sustain Brownian motion and can assemble into clusters. Hence, nucleation is better understood by investigating the geometry of clusters comprising isotropic nanoparticles than the geometry of atomic clusters.[8] On the other hand, self-assembly of anisotropic nanoparticles such as Janus, patchy, and multicompartment particles opens a pathway for creating new materials.[1,9] In recent years, many scientists have been attracted to this field of study. Since Zhang and Glotzer simulated the self-assembly of patchy particles, much effort has been exerted to the investigation of the self-assembly of patchy particles in simulation and theory.[10,11] With respect to experiment, Chen et al. studied the supracolloidal reaction kinetics of Janus spheres and made colloidal kagome lattice crystals from self-assembly of particles with two patches at opposite poles.[12] Gangwal et al. represented structures formed from patchy metallodielectric particles under high-frequency alternating current electric fields.[13] However, the build up of hierarchies requires precise control of the subunits that order into the next higher level.

Received: April 12, 2012
Revised: July 15, 2012
Published: July 17, 2012

   dx.doi.org/10.1021/la3014943 | *Langmuir* 2012, 28, 11714−11724

Consequently, great effort has been exerted to fabrication of subunits, i.e., patchy nanoparticles with precisely controlled patches.

In the past decades, many methods of patchy particle fabrication have been established. Pawar and Kretzschmar reviewed recent advances in this area. They highlighted six main techniques for fabricating patchy particles, such as (a) templating, (b) colloidal assembly, (c) particles lithography, (d) glancing-angle deposition, (e) nanosphere lithography, and (f) capillary fluid flow.[14] Apart from these methods, self-assembly of block copolymers is another promising route to prepare patchy particles.[15] For example, Janus particles, which can be regarded as the simplest patchy particle with only one patch, can be fabricated by self-assembly of block copolymers in bulk, confined environment, and solution. Hamburger-like and other patchy micelles formed by self-assembly of block copolymers in solution can be regarded as patchy particles with two and more patches, respectively. They are also multicompartment micelles whose solvophobic core can be further divided into distinct nanoscopic subdomains.

Multicompartment micelles, which sometimes feature patchy particles, are formed from self-assembly of amphiphilic block copolymers with at least two distinct solvophobic blocks or blends of copolymers in selective solvents. ABC miktoarm star copolymers, exemplified by Lodge and co-workers, can form a variety of fascinating multicompartment micelles, including laterally nanostructured vesicles, bowl-shaped semivesicles, polygonal-shaped bilayer sheets, segmented wormlike micelles, hamburger micelles, and raspberry micelles.[16] Multicompartment micelles can also be formed from linear block copolymers, such as ABCBA pentablock,[17] ABCA tetrablock,[18] and ABC triblock.[19] Very recently, Gröschel et al. generated a series of well-defined multicompartment micelles with precisely tunable patchiness by controlling the volume ratio of core-forming blocks in the linear ABC triblock copolymers.[20] They also demonstrated the hierarchical step-growth polymerization of these preassembled multicompartment micelles into micrometer-scale segmented supracolloidal polymers. Multicompartment micelles have been observed or predicted to form in blends of ABC star terpolymers and AB or ABC linear block copolymers[21−23] or in blends of two different diblock copolymers.[24] Nevertheless, making multicompartment micelles with precisely controlled number and location of patches on the surface of nanoparticles is still a challenging task for experimental researchers. This is because there are a larger number of influencing factors involved in self-assembly of ABC terpolymers in selective solvents.

In the present work, patchy multicompartment micelles formed from solution-state self-assembly of amphiphilic ABC linear terpolymers are investigated using computer simulations. A rich variety of patchy multicompartment micelles are formed spontaneously from a randomly generated initial configuration. In particular, a host of patchy and patchy-like multicompartment micelles with symmetric patches are predicted. The effects of the volume ratio of the solvophobic blocks, incompatibility between the two solvophobic blocks, and copolymer concentration on the patchy micellar morphologies are examined systematically. The dependence of the shape, number, and location of the patches in the resulting patchy micelles on the above parameters is elucidated. The simulation results may aid in fabricating polymeric nanoparticles with many patches that can precisely control their size, shape, number, and location.

MODEL AND METHOD

The simulated annealing method, a well-known procedure for obtaining the low-energy stable states in complex systems, is performed in the computer simulations.[25] The single-site bond fluctuation model of Carmesin and Kremer and of Larson is used to present the polymers in the model system.[26,27] The combination of the lattice model and simulated annealing method is efficient for studying the self-assembly of block copolymers in confined environments[28] or in solutions.[29] For completeness, the model and algorithm are briefly reviewed below, whereas a detailed description can be found elsewhere.[29]

In a simple cubic lattice of volume $V = L \times L \times L$ with $L = 60$, the periodic boundary condition is applied to all three directions and the polymers and solvents are embedded. The triblock copolymers consist of linear chains composed of A, B, and C monomers, $A_{NA}B_{NB}C_{NC}$ and $N = N_A + N_B + N_C$, where N_A, N_B, N_C, and N are the number of A, B, and C monomers as well as that of all monomers, respectively. Each monomer occupies one lattice site, and no two monomers can simultaneously occupy the same site, which is the self-avoiding model of terpolymers. Two consecutive monomers in a chain are connected by bonds that can adopt the length of 1 or $\sqrt{2}$; thus, each lattice site has 18 nearest neighbor sites. In each simulation, the initial configuration is generated by randomly creating N_{Ch} triblock copolymer chains on the lattice. After the desired number of terpolymer chains is generated, the unoccupied sites are designated as solvents where each solvent molecule occupies one lattice site. Only the exchange movement of monomers is used in the simulations. In an exchange move, a randomly selected monomer can exchange with a solvent molecule on one of its 18 nearest neighbors. The exchange is allowed if it does not break the terpolymer molecule. If a single break is created in the molecule, the vacancy continues to exchange with subsequent monomers along the broken chain until the links reconnect. The exchange is not allowed if it breaks the molecule into more than two parts. The Metropolis rule further governs the acceptance or rejection of an attempted move.[30]

The objective function of the simulated annealing procedure is the energy of the system. This work only considers the 18 nearest neighbor interactions, which are modeled by assigning an energy $E_{ij} = \varepsilon_{ij} k_B T_{ref}$ to each nearest neighbor pair of unlike components i and j, where $i, j = A, B, C$, and S (solvent), ε_{ij} is the reduced interaction energy between components i and j, k_B is the Boltzmann constant, and T_{ref} is the reference temperature. It is assumed that $\varepsilon_{ii} = 0$, with $i = A$, B, C, and S.

Simulations were carried out using a linear annealing schedule, $T_i = f\,T_{i-1}$, where T_i is the temperature used in the ith annealing step and f is a scaling factor. The annealing continues until the number of annealing steps reaches a predetermined value. The initial temperature is set at $T_1 = 120 T_{ref}$, and 130 annealing steps are used. At each annealing step, 9000 Monte Carlo steps (MCSs) are performed. One MCS is defined as, on average, all the lattice sites to be visited for an attempted move. Considering that the polymer concentration is very low in the systems considered in the present paper, each chain monomer, on average, can be visited a large number of times at each annealing. The scaling factor f is taken as 0.95 when the difference of the average energy of the system at the previous two annealing steps is smaller than a predetermined value; otherwise, $f = 0.99$.

In this study, all terpolymers employed in the simulations consist of two solvophobic (A and B) blocks and one solvophilic (C) block. The chain length of the terpolymer is fixed at $N = 24$, whereas the length of the C block is fixed at $N_C = 4$. We only focus on the case where the end solvophobic A block is less insoluble than the middle solvophobic B block. Under this condition, these ABC terpolymers are more likely to form patchy multicompartment nanoparticles, as discussed in the following sections. Therefore, the amphiphilic nature of chains is enforced by keeping $\varepsilon_{AS} = 2$, $\varepsilon_{BS} = 3$, $\varepsilon_{CS} = -1$, and $\varepsilon_{AC} = \varepsilon_{BC} = 1$ constant. This set of interaction parameters ensures that the solvent is poor to the A and B blocks but good to the C block and that the A or B and C blocks are immiscible. The two solvophobic blocks are also immiscible, i.e., $\varepsilon_{AB} > 0$. The phase space is explored by varying the

dx.doi.org/10.1021/la3014943 | Langmuir 2012, 28, 11714−11724

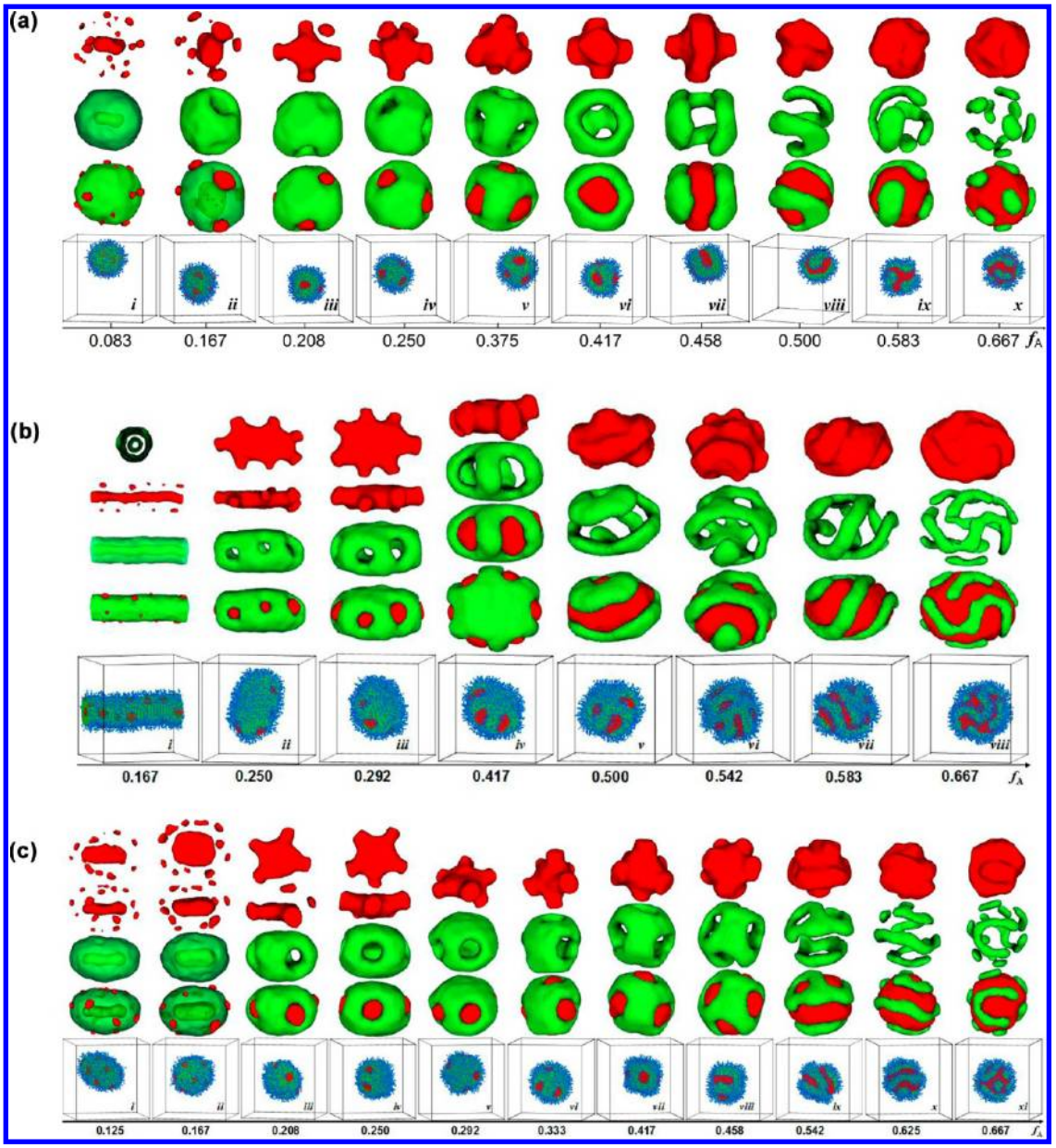

Figure 1. Typical morphologies of ABC linear terpolymers in selective solvents for the end C block as a function of the volume fraction of A block (f_A) at copolymer concentrations of c_p = (a) 0.04, (b) 0.08, and (c) 0.06 and $\varepsilon_{AB} = \varepsilon_{AS} = 2.0$. For clarity, a micellar structure in which the C blocks are removed and views with A or B domains only are shown above the corresponding snapshot. (a) Labels correspond to (*i*) core−shell−corona micelles, (*ii*−*vii*) patchy-like micelles, (*viii*−*ix*) ribbon−shell micelles, and (*x*) patchy micelles. (b) Labels correspond to (*i*) core−shell−corona micelles, (*ii*−*iv*) patchy-like micelles, and (*v*−*viii*) ribbon−shell micelles. (c) Labels correspond to (*i*, *ii*) core−shell−corona micelles, (*iii*−*viii*) patchy-like micelles, and (*ix*−*xi*) ribbon−shell micelles. Color scheme: A (red), B (green), C (blue).

block lengths N_A or equivalently the volume fraction $f_A = N_A/N$ (notice that f_B is changing with f_A) and the copolymer solution concentration. The copolymer concentration is defined as $c_p = NN_{Ch}/V$, where N_{Ch} is the number of copolymer chains in the system. On the other hand, the effects of the incompatibility between two solvophobic blocks on the micellar morphology are examined by varying the interaction parameter ε_{AB} at different f_A values. Finally, the reasons for micellar formation and morphological transitions are discussed.

RESULTS AND DISCUSSION

In this section, the simulation results are presented in the form of morphological phase diagrams. The results are also discussed and compared with previous experimental, theoretical, and simulation results. The phase diagrams in terms of the volume fraction of *A* block (f_A) only, or in terms of f_A and the copolymer concentration (c_p) for a given set of interaction parameters (Figures 1 and 2), or in terms of f_A and the interaction parameter ε_{AB} (Figure 3) for a given copolymer concentration are shown first. The mechanisms of morphological transition with increasing f_A and c_p are then elucidated by computing the contact numbers between different species as a function of f_A (Figure 4). The configuration and packing of chains in different micelles are investigated by calculating the mean square end-to-end distance (Figure 5) and distribution of angles between the vectors from the center of mass of the middle B block to the centers of mass of the A and C blocks of a terpolymer (Figure 6). Simulation results are compared with those obtained when the solvophilic C block is removed from the terpolymer (Figure 7).

dx.doi.org/10.1021/la3014943 | *Langmuir* 2012, 28, 11714−11724

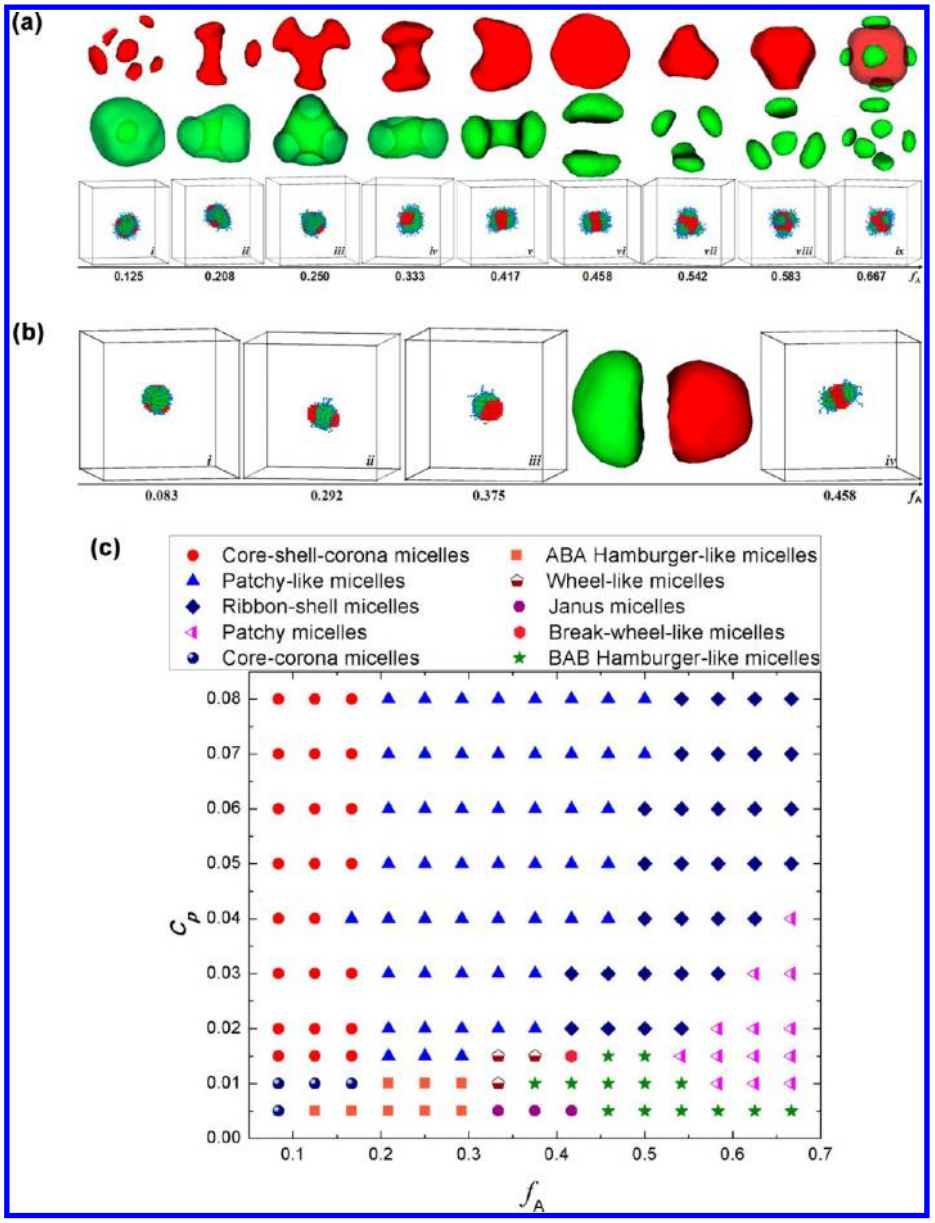

Figure 2. (a and b) Typical morphologies of ABC linear terpolymers in selective solvents for the end C block as a function of f_A when c_p = (a) 0.015 and (b) 0.005. Color code is the same as that in Figure 1. (a) Labels correspond to (*i*) core−shell−corona micelles, (*ii*, *iv*) wheel-like micelles (or patchy-like micelles), (*iii*) patchy-like micelles, (*v*) break−wheel-like micelles (or ribbon−shell micelles), (*vi*) hamburger-like micelles, and (*vii*−*ix*) patchy micelles. (b) Labels correspond to (*i*) core−corona micelles, (*ii*) hamburger-like micelles (A−B−A), (*iii*) Janus micelles, and (*iv*) hamburger-like micelles. (c) Morphological phase diagram of ABC linear terpolymers in selective solvents as a function of f_A and c_p with $\varepsilon_{AB} = \varepsilon_{AS} = 2.0$. Same symbols represent the same morphologies. For clarity and convenience, representative snapshots of the micellar morphologies are not shown.

Morphological Phase Diagram As a Function of Terpolymer Composition and Concentration. In Figure 1a, a morphological sequence, from core−shell−corona micelles (*i*) → patchy-like micelles (*ii*−*vii*) → ribbon−shell micelles (*viii*,*ix*) → patchy micelles (*x*), is observed with increased f_A at a given copolymer concentration c_p = 0.04. In the core−shell−corona micelles, a core and many small domains consisting of A blocks are located inside and outside a shell formed from B blocks. The corona formed by the solvophilic *C* blocks is on the surface of the micelle. On the other hand, the number of patches in patchy-like micelles varies with increased f_A. With increased f_A, one patch is formed first by connecting the core and domain comprising *A* blocks on the surface of micelles (*ii*). As a result, the shell has one hole. As the value of f_A increases, more patches appeare and distribute with high symmetry in the micelles (*iii*−*vi*). At the same time, the shell has more holes and finally resembles a cage. The patches progressively enlarge with increased f_A. However, when f_A reaches 0.458, the number of patches drops rapidly to two as shown in Figure 1a (*vii*). In that micelle, the shell becomes a bent toroid (or bent wheel). When f_A is larger than 0.458, the ribbon−shell micelles are observed (*viii*, *ix*). The length of ribbons fromed by B blocks shortens with increased f_A. Finally, the patchy micelles emerge in the morphological sequence comprising a big core formed from A blocks, many relative small domains consisting of B blocks pasted on the core surface, and a small corona composed of C blocks grafting on the B domains and dispersing in solvents. Hence, patchy micelle can also be regarded as patchy nanoparticle with a solvophobic core and solvophilic patches. In previous experi-

dx.doi.org/10.1021/la3014943 | *Langmuir* 2012, 28, 11714−11724

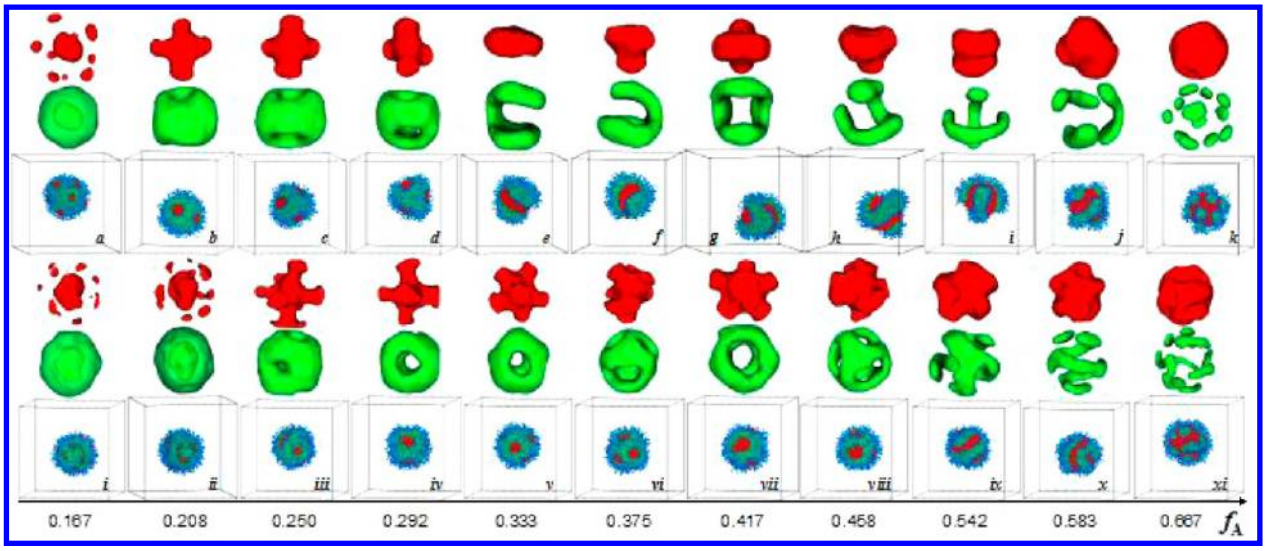

Figure 3. Typical morphologies of ABC linear terpolymers in selective solvents for the end C block as a function of f_A with ε_{AB} = 4.0 (top row) and 1.0 (bottom row) and c_p = 0.04. ε_{AS} is fixed at 2.0. Color scheme is the same as that in Figure 1.

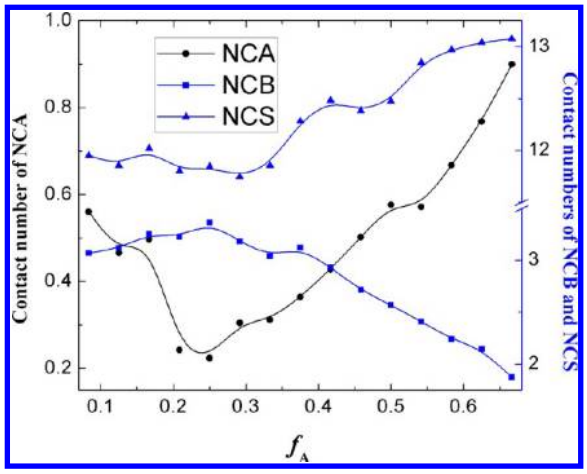

Figure 4. Variation in the average contact numbers for each C monomer with varying f_A in the case of ε_{AB} = ε_{AS} = 2.0 and c_p = 0.04.

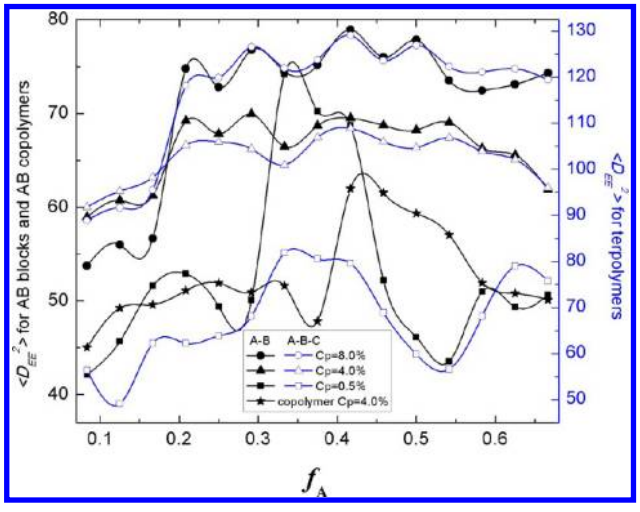

Figure 5. Variation of the mean square end-to-end distance ($\langle D_{EE}^2 \rangle$) of ABC terpolymers (blue curves with open symbols), AB blocks of terpolymers (black curves with solid squares, triangles, and dots), and AB diblock copolymers (black curve with solid star) with varying f_A.

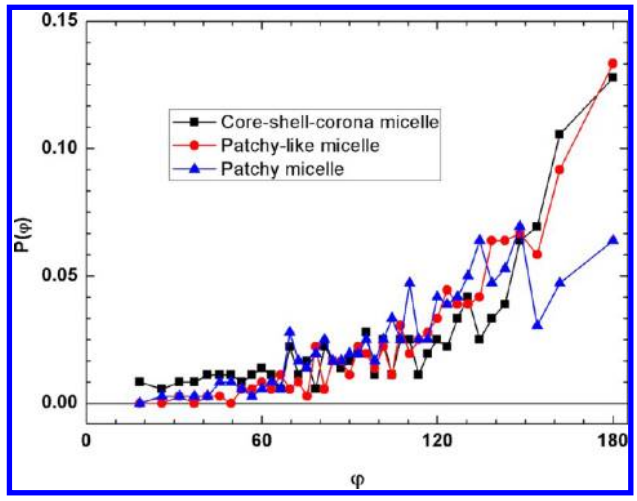

Figure 6. Distribution $P(\varphi)$ for triblock copolymers $A_2B_{18}C_4$, $A_{10}B_{10}C_4$, and $A_{16}B_4C_4$ in the core−shell−corona, patchy-like, and patchy micelles, respectively, when c_p = 0.04.

ments, patchy micelles were observed frequently. They can be formed not only from linear ABC triblock copolymers but also from ABC miktoarm star copolymers consisting of two solvophobic blocks and one solvophilic block.[16,31] Many micelles shown in Figure 1a were also predicted by previous simulations, although they were formed from different copolymers. For example, the solvophobic domain morphologies of our patchy micelles agree with the patchy nanoparticles discovered by Zhang et al. in their coarse-grain molecular dynamics simulation.[32] In their study, the influence of the number of repeated units (n) and other factors on the morphology of the aggregate formed from single-chain $(A-B)_n$ multiblock copolymer in poor solvents was studied while keeping the length of segments A−B constant. Holmes and Williams performed a self-consistent field theory simulation to investigate the aggregation of single-chain multiblock copolymer composed of alternating A and B blocks in poor solvent.[33] They found many patchy colloids similar to the solvophobic domains of our micelles, including patchy-like micelles with three patches, ribbon−shell micelles, patchy micelles, and so

dx.doi.org/10.1021/la3014943 | Langmuir 2012, 28, 11714−11724

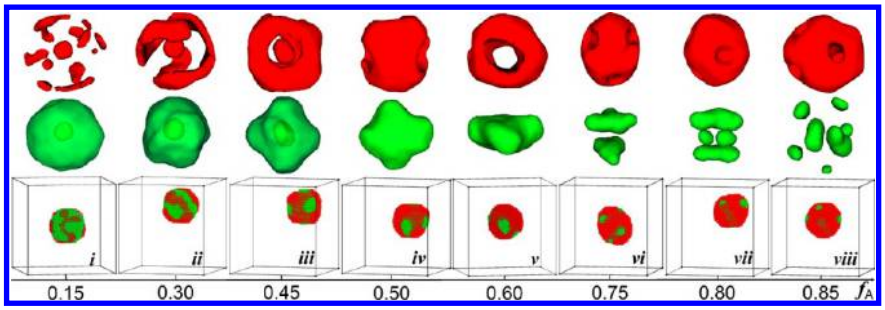

Figure 7. Typical morphologies of the diblock copolymers in a poor solvent for both A and B blocks as a function of f_A when the length and number of AB diblock copolymers in each aggregate are equal to that in Figure 1a. Color scheme is the same as that in Figure 1.

forth. Using dissipative particle dynamics simulation, Lin et al. investigated the structural evolution of multicompartment micelles self-assembled from linear ABC triblock copolymers in selective solvents.[34] They found that the concentric core−shell−corona structures transform into a C−bump−B micellar structure with decreased solubility of B blocks or into a B−bump−C micellar structure with decreased the length of B blocks. The C−bump−B micelle and B−bump−C micelle they obtained agree well with the core−shell−corona micelle and patchy micelle achieved in the current work, respectively. From the tendency of morphological transition, transformation of the patchy micelles into core−corona micelles in an extremely arduous condition is easy to imagine. Under this condition, the middle block disappears and the amphiphilic terpolymer becomes diblock copolymer.

Figure 1b shows the morphological sequence of micelles formed in solution at a relatively high copolymer concentration (c_p = 0.08). A comparison of the micellar morphologies with those shown in Figure 1a reveals many differences, although the tendency of morphological transition in two sequences is similar. First, the core and micelle are not spherical anymore and instead become cylindrical for the core−shell−corona micelles (*i*). Second, for the patchy-like micelles (*ii*−*iv*), the core and micelle become oblate and the patches locate on the edge of the flat patchy-like micelles. With increased f_A, the core progressively thickens and consequently the patches progressively enlarge. Jiang and co-workers observed bump surface multicompartment micelles experimentally in their studies of the self-assembly of polystyrene-*b*-polybutadiene-*b*-poly (2-vinylpridine) linear terpolymers in mixtures of toluene and methanol, and they reproduced these micelles using self-consistent field theory simulations.[35] The discoidal micelle in their work is in good agreement with the oblate patchy-like micelle obtained in the present work. Third, with increased f_A, the ribbons formed from B blocks narrow in size and shorten in length in the ribbon−shell micelles (*v*−*viii*). The micellar shape changes into prolate ellipsoidal from oblate. Finally, the sequence lacks in patchy micelles.

The morphological sequence shown in Figure 1c is also from core−shell−corona micelles → patchy-like micelles → ribbon−shell micelles with increased f_A at an intermediate concentration of copolymers (c_p = 0.06). Comparing Figure 1c and 1b reveals that there is no patchy micelle in both sequences and that the differences between them are also obvious. The core and micelle are ribbon-like and ellipsoidal, respectively, instead of cylindrical for core−shell−corona micelles (*i*). With increased f_A, the core and micelle change into disk-like and somewhat oblate (*ii*) from ribbon-like and ellipsoidal, respectively. In ribbon−shell micelles (*ix*−*xi*), although the ribbon lengths in both figures shorten, the micelles shown in Figure 1c stay spherical, with increased f_A. With increased f_A, the patchy-like micelles (*iii*−*viii*) change into spherical from oblate, the location of patches becomes three-dimensional from the rim of micelles, and the micellar cores also become three-dimensional from flat. On the other hand, there are also many differences between Figure 1c and 1a. The sequence in Figure 1c lacks patchy micelles. There is no ellipsoidal micelle with a ribbon-like core for the core−shell−corona micelles shown in Figure 1a. With increased f_A, all micelles in Figure 1a are spherical but the micelles change into spherical from ellipsoidal in Figure 1c.

In the current study, we also examined the self-assembly of ABC terpolymers in a very dilute solution ($c_p \leq 0.015$). In Figure 2a (c_p = 0.015) and 2b (c_p = 0.005), the morphological sequences and transitions of micelles clearly differ from those shown in Figure 1. For instance, when c_p = 0.015 (Figure 2a), the overall tendency of morphological transition and variation of the number of patches with f_A in the patchy-like micelles are similar to those shown in Figure 1. However, the number of patches becomes small even in the micelle (*iii*) that has the most patches in micellar sequence. Wheel-like (*iv*), break−wheel-like (*v*), and hamburger-like (*vi*) micelles are observed instead of patchy-like, ribbon−shell, and patchy micelles in the morphological sequence. If the hamburger-like micelles formed by stacked disks in B−A−B sequence can be regarded as one of the special patchy micelles that have two linear symmetric caps on both ends, the morphological sequence of patchy micelles consists of micelles with symmetric two, three, four, and six patches on the surface of the micellar core formed from A blocks, and the center of each patch can be regarded as located on one of the vertices of a regular polyhedron. Notably, the symmetry decreases or even disappears in patchy micelles when they have much more caps. When c_p = 0.005, there is a morphological sequence composed of core−corona micelles (*i*), two different hamburger-like micelles (*ii*, *iv*), and Janus micelles (*iii*) in between both hamburger-like micelles shown in Figure 2b. The core of core−shell−corona micelles disappears, resulting in core−corona micelles with small domains formed from A blocks located on the surface of the core formed by B blocks. Srinivas and Pitera achieved a variety of soft patchy nanoparticles from the solution-phase self-assembly of binary blends of diblock copolymers with different ratios using coarse-grain molecular dynamics simulation.[24a] Although the soft patchy nanoparticles consist of AB and BC two diblock copolymers, the spherical patchy nanoparticles they observed are similar to the core−corona micelles (Figure 2b, *i*) obtained in the present study. As the small domains get together in two poles of a core, a new hamburger-like micelle with disks stacked

dx.doi.org/10.1021/la3014943 | *Langmuir* 2012, 28, 11714−11724

in an A−B−A order is observed in the morphological sequence. Janus micelle is composed of two hemispheres formed by A and B blocks, respectively. The C blocks grafted on the surface of the hemisphere formed by B blocks cause the Janus micelle to have solvophilic and solvophobic hemispheres. As a result, these Janus nanoparticles are amphiphilic and can be the building blocks of hierarchical multifunctional nanomaterials. However, a hamburger-like micelle with disks stacked in a B−A−B order is obtained with further increasing f_A (*iv*). Dupont and Liu observed hamburger-like micelles formed from poly(*tert*-butylacrylate)-*b*-poly(2-cinnamoyloxyethyl methacrylate)-*b*-poly(sucinnated glyceryl monomethacrylate) linear triblock copolymers in THF/propanol solvents.[36] Their observations agree with the B−A−B hamburger-like micelles in the present study. Using Wang−Landau Monte Carlo simulation, Parsons and Williams observed some aggregates from single-chain $(A-B)_n$ multiblock copolymer in poor solvents when they alter the length of A and B blocks simultaneously while keeping the total copolymer length constant.[37] The dicluster and triglobule they obtained are similar with the solvophobic domains of Janus and hamburger-like micelles in the present work, respectively. Zhu et al. applied the Monte Carlo method to study the self-assembly of linear ABC amphiphiles in C-selective solvents.[38] They reported hamburger micelles, worm-like micelles with bumps on the sides, and disk-like micelles with bumps on the edge. These micelles correspond to the B−A−B hamburger-like micelles (Figure 2a, *iv*), oblate patchy-like micelles (Figure 1b, *ii*), and flat patchy micelles (Figure 1b, *iv*), respectively, predicted in the current study, respectively.

To understand fully the effects of f_A and c_p on the morphology and morphological transition, the phase diagram of f_A and c_p for a given set of interaction parameters is shown in Figure 2c. For clarity and convenience, representative snapshots of micelles are given in Figures 1, 2a, and 2b. Although there are many differences among the micelles as discussed in previous sections, some generic common features of the phase behavior can be extracted from the phase diagram. First, the morphological sequences at different copolymer concentrations are similar, except those in extremely dilute solutions ($c_p \leq 0.01$). For example, with increased f_A, the internal structure of the micelles varies according to the following sequence: core−shell−corona structures → core with bumps−cage-like shell structures → core−ribbon-like shell structures → patchy structures. Second, with increased c_p, the shapes of the micellar core and micelle change in every micellar phase region. For example, for the core−shell−corona micelles, the shapes of the core and micelle are always spherical in low copolymer concentrations, whereas they become oblate, ribbon- or rod-like, and ellipsoidal or cylindrical at high copolymer concentrations. For patchy-like micelles, the spherical micelles also become ribbon-like or oblate with increased c_p. Apart from the number of patches in the micelles increasing with increased c_p, the symmetry of the location of patches is variable. A case in point is that the symmetry changes with the change in f_A in low and intermediate copolymer concentrations, whereas in high copolymer concentrations the patches are located on the edge of oblate and ribbon-like micelles. The length and number of ribbons increase with increased c_p in ribbon−shell micelles. Third, when c_p is large, the phase region of patchy-like and ribbon−shell micelles extends and shifts to larger f_A values, respectively. As a result, the phase of patchy micelles disappears in the high c_p region of the phase diagram. Finally, apart from the variety of morphologies and morphological transitions in the phase diagram, the volume of micelles enlarges with increased copolymer concentration. Thus, the final micellar morphology for a given set of interaction parameters depends sensitively not only on the copolymer compositions but also on the copolymer concentration of the systems (or, more accurately, on the number of copolymer chains in the micelles). In addition, it is worthy to note that a variety of micelles with disparate morphologies are also observed to coexist even in one experimental system.

Micelles Formed in the Case of ε_{AB} Unequal to ε_{AS}. All aforementioned micelles were obtained in a special case in which the incompatibility (ε_{AB}) of two solvophobic blocks and interaction (ε_{AS}) between *A* monomers and solvents are equivalent. To gain insight into the morphology of micelles with unequal ε_{AB} and ε_{AS}, we investigated the self-assembly of ABC terpolymers with $\varepsilon_{AB} < \varepsilon_{AS}$ and $\varepsilon_{AB} > \varepsilon_{AS}$, respectively. Two series of typical micellar morphologies as a function of f_A were gained, as shown in Figure 3. For the case of $\varepsilon_{AB} < \varepsilon_{AS}$ ($\varepsilon_{AB} = 1.0$, $\varepsilon_{AS} = 2.0$), although the morphological sequence is similar with the one shown in Figure 1a, there are many differences between them. First, the patchy micelles disappear because the ribbons tend to become narrow rather than shorten with increased f_A in ribbon−shell micelles (*ix*−*xi*). In patchy-like micelles (*iii*−*viii*), the number of patches is much larger (there are seven or six patches in each micelle) and remains constant with increased f_A. The location of patches is symmetric. On the other hand, when $\varepsilon_{AB} > \varepsilon_{AS}$ ($\varepsilon_{AB} = 4.0$, $\varepsilon_{AS} = 2.0$), the morphological sequence is also very different from the one shown in Figure 1a. For instance, the surface of the domains formed by A blocks is smoother. The patches are few in the patchy-like micelles (Figure 1b−d). A comparison of the morphologies and morphological transitions in Figures 3 and 1a reveal that the competition of the interfacial energy of polymer−polymer and polymer−solvent is one of the main factors determining micellar morphology.

Reasons for the Micellar Formation and Morphological Transition. Many morphologies and morphological transitions were predicted and compared with experimental, theoretical, and simulation results. However, the reasons for these micellar formation and morphological transitions are still unclear, which may hinder complete understanding of how to control precisely the size and shape of patchy nanoparticles. Therefore, we analyze the interfacial energy, the stretching energy of chains, and the influence of C blocks in the following subsections to reveal the reasons for micellar formation.

To gain insight into the effect of interfacial energy on micellar morphology and morphological transition, we calculated the average contact number among the species in the system. The nearest neighbors of a monomer are one of the four species, namely, the A monomer, B monomer, C monomer, and solvent. The total contact number for each monomer should be 18, which is equal to the number of nearest neighbors in our model. The average contact numbers for the C monomer with A monomers, B monomers, and solvents are denoted as NCA, NCB, and NCS, respectively. Figure 4 depicts the variations of the average contact number between C monomer and other species as a function of f_A for the morphologies shown in Figure 1a. Several generic features can be extracted from Figure 4. First, NCA is not equal to zero at any value of f_A, which indicates that there are always some A monomers located on the outside surface of the B shell. As a result, the A monomers can be seen directly in any micellar snapshots shown in Figures 1−3. There are two reasons. One is

that the interaction between B monomer and solvent (ε_{BS} = 3.0) is stronger than the one between A monomer and solvent (ε_{AS} = 2.0). The other is that when f_A is very small, the long B blocks prefer to coil themselves to maximize their entropy of chain conformation, which makes short A blocks to be located on the outside surface of the shell formed by B blocks. Due to the superiority of entropy loss to the decrease in energy caused by aggregation of A monomers, A monomers can only form small domains that lead to a relatively large value of NCA. In the other case, B monomers prefer aggregating into domains to enwrapping the big A domain, which leads to part of the surface of the A domain being exposed to solvents and C monomers. Second, the ratio of f_A and f_B causes variations in NCA, NCB, and NCS. When f_A is very small (f_A < 0.25), the increase in NCB and decrease in NCA and NCS with increased f_A indicate that some C monomers go to the interface of B−Solvent to decrease the interfacial energy of B domain and solvents. The influence of the entropy of B blocks becomes weak as they are short. Therefore, the decrease in energy induced by aggregation of A monomers due to elongation of A blocks dominates the micellar structures, resulting in many A blocks forming patches connecting the core instead of small domains on the outside surface of the shell. As a result, this morphological transition leads to the decrease in NCA and NCS as well as the increase in NCB. On the other hand, when f_A is larger than 0.25, the increase in NCA and decrease in NCB with increased f_A can lead to the deduction that more and more C monomers transform into the interface of A−Solvent from the interface of B−Solvent to reduce the interfacial energy of the interface of A−Solvent. This phenomenon can be attributed to the interfaces of B−Solvent and B−C becoming small while that of A−Solvent rapidly enlarges, which are caused by the decrease in B monomers and increase in A monomers with increased f_A. It is indicated that more C blocks disperse in solvents apart from those located at the interfaces of A−Solvent and B−Solvent from the increase in NCS. This phenomenon is due to sufficient C monomers at the interface between B domain and solvents to prevent their contact and to the C blocks being too short to reach the uncovered domain formed by A monomers. As a result, some C blocks disperse in solvents.

Besides interfacial energies, the stretching energy of the chain is another factor that determines the micellar structure and shape. Thus, the stretch of polymer chains is examined by calculating the mean square end-to-end distance ($\langle D_{EE}^2 \rangle$). Figure 5 shows the $\langle D_{EE}^2 \rangle$ values of ABC terpolymers and AB block segments for concentrations of 0.5%, 4.0%, and 8.0% as well as AB diblock copolymers with the same chain number as the ABC terpolymers at a concentration of 4.0% as a function of f_A. The $\langle D_{EE}^2 \rangle$ value of terpolymer chains increases with increased c_p or, more accurately, the number of terpolymers in micelles, except the $\langle D_{EE}^2 \rangle$ values for f_A < 0.2 at concentrations of 4.0% and 8.0% (the core−shell−corona micelle phase). The terpolymers are forced to coil themselves in the micelle with few chains (c_p = 0.5%), which results in a small $\langle D_{EE}^2 \rangle$ value of ABC terpolymers. The solvophilic block must be located on the micellar surface; thus, the entire copolymer cannot be located in the inner parts of micelle. Therefore, the solvophobic segments have to compress themselves to fill the internal space of micelles comprised of many chains (c_p= 4.0%), which leads to the large $\langle D_{EE}^2 \rangle$ value. It is easy to deduce that when micelles are larger than a certain value their shape is cylindrical or flat rather than spherical, as shown in Figure 1b (c_p = 8.0%). It is concluded that the $\langle D_{EE}^2 \rangle$ values of terpolymers are relatively small in core−shell−corona micelles, patchy micelles, core−corona micelles, and hamburger-like micelles but relatively large in patchy-like, ribbon−shell, and Janus micelles from the variation of $\langle D_{EE}^2 \rangle$ of terpolymers with varying f_A and the corresponding morphologies in the phase diagram shown in Figure 2c. Although the $\langle D_{EE}^2 \rangle$ values are small in both core−shell−corona micelles and patchy micelles, their reasons are different. Those features arise from the differences in the chain conformations.

To understand better the chain conformation in different micelles, the distributions of angles (φ) for some typical micelles are calculated. The angle is formed by the vectors from the center of mass of the middle B block to the center of mass of end blocks A and C. Figure 6 depicts the distributions of angles (φ) for the terpolymers in core−shell−corona micelles, patchy-like micelles, and patchy micelles. For a core−shell−corona micelle, many terpolymers with A, B, and C blocks forming the core, shell, and corona, respectively, have an extended conformation because terpolymers have relatively high distributions in the region of φ > 150°. However, there are also some terpolymer distributions in the region of φ < 60° that are also observed, indicating that the looped conformation also exists. This phenomenon is caused by the presence of some domains composed of A blocks on the surface of micelles. Thus, the small $\langle D_{EE}^2 \rangle$ value of loop terpolymers counteract the big $\langle D_{EE}^2 \rangle$ value of extended terpolymers, which results in a relatively small $\langle D_{EE}^2 \rangle$ value for core−shell−corona micelles. In patchy micelles, both looped (φ < 60°) and extended (φ > 150°) chains are fewer than those in the core−shell−corona micelle, which also leads to a relatively small $\langle D_{EE}^2 \rangle$ value. However, many extended (φ > 150°) and few looped (φ < 60°) terpolymers result in a large $\langle D_{EE}^2 \rangle$ value in patchy-like micelles.

In Figure 5, the variations in the $\langle D_{EE}^2 \rangle$ values of AB blocks and of the terpolymers with varying f_A are similar, except that the size of AB blocks is smaller than that of the terpolymers because the size of C blocks is not included. However, the $\langle D_{EE}^2 \rangle$ value of AB diblock copolymers differs from that of AB blocks in terpolymers when they are in the same copolymer concentration of 4% (or, more accurately, for the same number of copolymer chains in each micelle). The $\langle D_{EE}^2 \rangle$ value of AB diblock copolymers is shorter than that of AB blocks in terpolymers, and the variation of the former with varying f_A also differs from that of the latter, although the NA and NB values of AB diblock copolymers and those of AB blocks in terpolymers are identical at any value of f_A. These differences are attributed to the anchoring effects of *C* blocks in ABC terpolymers. The *C* blocks of terpolymers are solvophilic so that they are on the surface of micelles not only to shield the micellar core from contacting with solvents but also to make the join point between B and C blocks always locate at the interface of B−C. As a result, the chain packing and end-to-end distance of AB blocks are influenced, and micellar morphology is affected correspondingly.

To obtain an intuitive understanding of the anchoring effects of C blocks on micellar morphology, the morphologies of the micelles formed by AB diblock copolymers with the same chain number and the same interactions as those in Figure 1a are given in Figure 7. A comparison between Figures 1a and 7 reveals many differences, although the diblock copolymers just lack a solvophilic C block compared with the terpolymers. When f_A is small, the morphology of the aggregates (Figure 7, *i*) is similar to the solvophobic domain of the core−shell−corona

dx.doi.org/10.1021/la3014943 | *Langmuir* 2012, 28, 11714−11724

micelles (Figure 1a, *i*). However, the shell formed by B blocks is bilayered. As a result, the bilayer shell leads to the small $\langle D_{EE}^2 \rangle$ of AB diblock copolymers, as shown in Figure 5. With increased f_A, although the structure of aggregates does not change, the small domains formed from A blocks aggregate into ribbons, then into one long ribbon (*ii*), and finally into a cage on the surface of shell. As a result, patchy-like aggregates (*iii*) composed of core, shell, and network are formed. When f_A is intermediate, diblock copolymers self-assemble into inverse patchy micelles (*iv*, *v*) in which B blocks form the core with bumps and the shell consists of the A blocks. At the same time, the $\langle D_{EE}^2 \rangle$ value of AB diblock copolymers increases sharply because of the disappearance of the bilayer shell formed by B blocks. When f_A increases ($f_A \geq 0.75$), the systems form spherical aggregates (*vi*–*viii*) instead of ribbon–shell and patchy micelles and the B block domains disperse in a spherical matrix composed of A blocks. These differences are caused only by the lack of the anchoring effects of solvophilic C blocks. Part of AB diblock copolymers can fit in the inner parts of aggregates without anchoring of C blocks. Consequently, the chain conformation and packing are changed, which causes the change in the morphology of aggregates. Therefore, the solvophilic C block in terpolymers is an important factor that leads systems to self-assemble into highly symmetric patchy micelles, as shown in Figures 1–3.

CONCLUSION

Using a simulated annealing technique we investigated the self-assembly of amphiphilic ABC linear terpolymers in C-block-selective solvents. Various micellar structures with the features of patchy nanoparticles can be formed. These structures are different from traditional morphologies such as spheres, cylinders, disks, and vesicles in previous work. These patchy nanoparticles are highly symmetric and can be outstanding building blocks for hierarchical multifunctional nanomaterials. Phase diagrams and morphological transitions are obtained by controlling the copolymer composition, copolymer concentration, and incompatibility between the solvophobic blocks under a proper condition. By calculating and analyzing the contact number between species, mean square end-to-end distances of the terpolymers, of the AB block chains in the terpolymers, and of the AB diblock copolymers, distribution of angle of terpolymers in typical micelles, as well as comparing the morphologies formed from ABC triblock and AB diblock copolymers, the effects of these controlling factors on micellar morphology and morphological transition are elucidated.

Despite a variety of micellar morphologies and morphological transitions in the phase diagrams, several generic features are obtained. The volume ratio of the solvophobic blocks and the incompatibility between them mainly control the shape, number, and location of the patches in the resulting micelles. However, the overall geometry of a micelle is largely controlled by the copolymer concentration. With increased copolymer concentration, the micellar shape changes from spherical to cylindrical and/or oblate. On the other hand, ε_{BS} is larger than ε_{AS} and the anchoring effect of the C block are important factors leading the systems to form the micelles predicted in this article.

AUTHOR INFORMATION

Corresponding Author

*E-mail: ytzhu@ciac.jl.cn (Y.Z.); baohui@nankai.edu.cn (B.L.).

Notes

The authors declare no competing financial interest.

ACKNOWLEDGMENTS

This work was supported by the China Postdoctoral Science Foundation (20100481071), National Science Fund for Distinguished Young Scholars of China (20925414), National Natural Science Foundation of China for Youth Science Funds (21104083), General Program (20990234), Major Program (50930001), Creative Research Groups (50621302), and Scientific Development Program of Jilin Province (201201007).

REFERENCES

(1) Glotzer, S. Some Assembly Required. *Science* **2004**, *306*, 419–420.

(2) Park, M.; Harrison, C.; Chaikin, P. M.; Register, R. A.; Adamson, D. H. Block Copolymer Lithography: Periodic Arrays of ~10^{11} Holes in 1 Square Centimeter. *Science* **1997**, *276*, 1401–1404.

(3) Collier, J. H.; Messersmith, P. B. Phospholipid strategies in biomineralization and biomaterials research. *Annu. Rev. Mater. Res.* **2001**, *31*, 237–263.

(4) Savić, R.; Luo, L.; Eisenberg, A.; Maysinger, D. Micellar Nanocontainers Distribute to Defined Cytoplasmic Organelles. *Science* **2003**, *300*, 615–618.

(5) S. Auer, A. C.; Frenkel, D. Onset of heterogeneous crystal nucleation in colloidal suspensions. *Nature* **2004**, *428*, 404–406.

(6) Klix, C. L.; Royall, C. P.; Tanaka, H. Structural and Dynamical Features of Multiple Metastable Glassy States in a Colloidal System with Competing Interactions. *Phys. Rev. Lett.* **2010**, *104*, 165702–4.

(7) Johnston, R. L. *Atomic and Molecular Clusters*; Taylor & Francis: New York, 2002.

(8) Meng, G.; Arkus, N.; Brenner, M. P.; Manoharan, V. N. The Free-Energy Landscape of Clusters of Attractive Hard Spheres. *Science* **2010**, *327*, 560–563.

(9) Romano, F.; Sciortino, F. Patchy from the bottom up. *Nat. Mater.* **2011**, *10*, 171–173.

(10) (a) Zhang, Z.; Glotzer, S. Self-Assembly of Patchy Particles. *Nano Lett.* **2004**, *4*, 1407–1413. (b) Zhang, Z.; Keys, A. S.; Chen, T.; Glotzer, S. Self-Assembly of Patchy Particles into Diamond Structures through Molecular Mimicry. *Langmuir* **2005**, *21*, 11547–11551. (c) Glotzer, S.; Solomon, M. Anisotropy of building blocks and their assembly into complex structures. *Nat. Mater.* **2007**, *6*, 557–562.

(11) (a) Sciortino, F.; Bianchi, E.; Douglas, J.; Tartaglia, P. Self-assembly of patchy particles into polymer chains: A parameter-free comparison between Wertheim theory and Monte Carlo simulation. *J. Chem. Phys.* **2007**, *126*, 194903–10. (b) Noya, E. G.; Vega, C.; Doye, J.; Louis, A. The stability of a crystal with diamond structure for patchy particles with tetrahedral symmetry. *J. Chem. Phys.* **2010**, *132*, 234511–13. (c) Russo, J.; Tavares, J.; Teixeira, P.; Gama, M.; Sciortino, F. Re-entrant phase behaviour of network fluids: A patchy particle model with temperature-dependent valence. *J. Chem. Phys.* **2011**, *135*, 034501–13. (d) Heras, D.; Tavares, J.; Gama, M. Phase diagrams of binary mixtures of patchy colloids with distinct numbers of patches: the network fluid regime. *Soft Matter* **2011**, *7*, 5615–5626.

(12) (a) Chen, Q.; Whitmer, J. K.; Jiang, S.; Bae, S.; Luijten, E.; Granick, S. Supracolloidal Reaction Kinetics of Janus Spheres. *Science* **2011**, *331*, 199–202. (b) Chen, Q.; Bae, S.; Granick, S. Directed self-assembly of a colloidal kagome lattice. *Nature* **2011**, *469*, 381–385.

(13) Gangwal, S.; Pawar, A.; Kretzschmar, I.; Velev, O. Programmed assembly of metallodielectric patchy particles in external AC electric fields. *Soft Matter* **2010**, *6*, 1413–1418.

(14) Pawar, A.; Kretzschmar, I. Fabrication, Assembly, and Application of Patchy Particles. *Macromol. Rapid Commun.* **2010**, *31*, 150–168.

(15) (a) Hamley, I. W. *The Physics of Block Copolymers*; Oxford University Press: New York, 1998. (b) Hamley, I. W. *Block Copolymers in Solution: Foundamentals and Applications*; Wiley: New York, 2005; (c) Du, J.; Armes, S. P. Patchy multi-compartment micelles are formed

by direct dissolution of an ABC triblock copolymer in water. *Soft Matter* **2010**, *6*, 4851−4857.
(16) (a) Li, Z.; Kesselman, E.; Talmon, Y.; Hillmyer, M. A.; Lodge, T. P. Multicompartment Micelles from ABC Miktoarm Stars in Water. *Science* **2004**, *306*, 98−101. (b) Li, Z.; Hillmyer, M. A.; Lodge, T. P. Laterally Nanostructured Vesicles, Polygonal Bilayer Sheets, and Segmented Wormlike Micelles. *Nano Lett.* **2006**, *6*, 1245−1249. (c) Li, Z.; Hillmyer, M. A.; Lodge, T. P. Morphologies of Multicompartment Micelles Formed by ABC Miktoarm Star Terpolymers. *Langmuir* **2006**, *22*, 9409−9417. (d) Saito, N.; Liu, C.; Lodge, T. P.; Hillmyer, M. A. Multicompartment Micelles from Polyester-Containing ABC Miktoarm Star Terpolymers. *Macromolecules* **2008**, *41*, 8815−8822. (e) Liu, C.; Hillmyer, M. A.; Lodge, T. P. Evolution of Multicompartment Micelles to Mixed Corona Micelles Using Solvent Mixtures. *Langmuir* **2008**, *24*, 12001−12009. (f) Liu, C.; Hillmyer, M. A.; Lodge, T. P. Multicompartment Micelles from pH-Responsive Miktoarm Star Block Terpolymers. *Langmuir* **2009**, *25*, 13718−13725. (g) Saito, N.; Liu, C.; Hillmyer, M. A.; Lodge, T. P. Multicompartment Micelle Morphology Evolution in Degradable Miktoarm Star Terpolymers. *ACS Nano* **2010**, *4*, 1907−1912.
(17) Thünemann, A. F.; Kubowicz, S.; von Berlepsch, H.; Möhwald, H. Two-Compartment Micellar Assemblies Obtained via Aqueous Self-Organization of Synthetic Polymer Building Blocks. *Langmuir* **2006**, *22*, 2506−2510.
(18) (a) Brannan, A. K.; Bates, F. S. ABCA Tetrablock Copolymer Vesicles. *Macromolecules* **2004**, *37*, 8816−8819. (b) Gomez, E. D.; Rappl, T. J.; Agarwal, V.; Bose, A.; Schmutz, M.; Marques, C. M.; Balsara, N. P. Platelet Self-Assembly of an Amphiphilic A-B-C-A Tetrablock Copolymer in Pure Water. *Macromolecules* **2005**, *38*, 3567−3570.
(19) (a) Yu, G.; Eisenberg, A. Multiple Morphologies Formed from an Amphiphilic ABC Triblock Copolymer in Solution. *Macromolecules* **1998**, *31*, 5546−5549. (b) Gohy, J.-F.; Willet, N.; Varshney, S.; Zhang, J.-X.; Jérôme, R. Core - Shell - Corona Micelles with a Responsive Shell. *Angew. Chem., Int. Ed.* **2001**, *40*, 3214−3216. (c) Zhou, Z.; Li, Z.; Ren, Y.; Hillmyer, M. A.; Lodge, T. P. Micellar Shape Change and Internal Segregation Induced by Chemical Modification of a Tryptych Block Copolymer Surfactant. *J. Am. Chem. Soc.* **2003**, *125*, 10182−10183. (d) Lodge, T. P.; Hillmyer, M. A.; Zhou, Z.; Talmon, Y. Access to the Superstrong Segregation Regime with Nonionic ABC Copolymers. *Macromolecules* **2004**, *37*, 6680−6682. (e) Pochan, D. J.; Chen, Z.; Cui, H.; Hales, K.; Qi, K.; Wooley, K. L. Toroidal Triblock Copolymer Assemblies. *Science* **2004**, *306*, 94−97. (f) Zhu, J.; Jiang, W. Self-Assembly of ABC Triblock Copolymer into Giant Segmented Wormlike Micelles in Dilute Solution. *Macromolecules* **2005**, *38*, 9315−9323. (g) Li, Z.; Chen, Z.; Cui, H.; Hales, K.; Qi, K.; Wooley, K. L.; Pochan, D. J. Disk Morphology and Disk-to-Cylinder Tunability of Poly(Acrylic Acid)-*b*-Poly(Methyl Acrylate)-*b*-Polystyrene Triblock Copolymer Solution-State Assemblies. *Langmuir* **2005**, *21*, 7533−7539. (h) Chen, Z.; Cui, H.; Hales, K.; Li, Z.; Qi, K.; Pochan, D. J.; Wooley, K. L. Unique Toroidal Morphology from Composition and Sequence Control of Triblock Copolymers. *J. Am. Chem. Soc.* **2005**, *127*, 8592−8593. (i) Fustin, C.-A.; Abetz, V.; Gohy, J.-F. Triblock terpolymer micelles: A personal outlook. *Eur. Phys. J. E* **2005**, *16*, 291−302.
(20) Gröschel, A. H.; Schacher, F. H.; Schmalz, H.; Borisov, O. V.; Zhulina, E. B.; Walther, A.; Müller, A. H. E. Precise hierarchical self-assembly of multicompartment micelles. *Nat. Commun.* **2012**, *3*, NO. 710.
(21) Ma, J. W.; Li, X.; Tang, P.; Yang, Y. L. Self-Assembly of Amphiphilic ABC Star Triblock Copolymers and Their Blends with AB Diblock Copolymers in Solution: Self-Consistent Field Theory Simulations. *J. Phys. Chem. B* **2007**, *111*, 1552−1158.
(22) Li, Z.; Hillmyer, M. A.; Lodge, T. P. Control of Structure in Multicompartment Micelles by Blending μ-ABC Star Terpolymers with AB Diblock Copolymers. *Macromolecules* **2006**, *39*, 765−771.
(23) Xin, J.; Liu, D.; Zhong, C. Multicompartment Micelles from Star and Linear Triblock Copolymer Blends. *J. Phys. Chem. B* **2007**, *111*, 13675−13682.
(24) (a) Srinivas, G.; Pitera, J. W. Soft Patchy Nanoparticles from Solution-Phase Self-Assembly of Binary Diblock Copolymers. *Nano Lett.* **2008**, *8*, 611−618. (b) Zhu, J.; Hayward, R. C. Wormlike Micelles with Microphase-Separated Cores from Blends of Amphiphilic AB and Hydrophobic BC Diblock Copolymers. *Macromolecules* **2008**, *41*, 7794−7797.
(25) (a) Kirkpatrick, S.; Gelatt, C. D.; Vecchi, M. P., Jr. Optimization by Simulated Annealing. *Science* **1983**, *220*, 671−680. (b) Grest, G. S.; Soukoulis, C. M.; Levin, K. Cooling-Rate Dependence for the Spin-Glass Ground-State Energy: Implications for Optimization by Simulated Annealing. *Phys. Rev. Lett.* **1986**, *56*, 1148−1151.
(26) Carmesin, I.; Kremer, K. The Bond Fluctuation Method: A New Effective Algorithm for the Dynamics of Polymers in All Spatial Dimensions. *Macromolecules* **1988**, *21*, 2819−2823.
(27) (a) Larson, R. G. Self-assembly of surfactant liquid crystalline phases by Monte Carlo simulation. *J. Chem. Phys.* **1989**, *91*, 2479−2488. (b) Larson, R. G. Monte Carlo simulation of micro-structural transitions in surfactant systems. *J. Chem. Phys.* **1992**, *96*, 7904−7918.
(28) Yu, B.; Sun, P.; Chen, T.; Jin, Q.; Ding, D.; Li, B.; Shi, A.-C. Confinement-Induced Novel Morphologies of Block Copolymers. *Phys. Rev. Lett.* **2006**, *96*, 138306−4.
(29) (a) Sun, P.; Yin, Y.; Li, B.; Chen, T.; Jin, Q.; Ding, D.; Shi, A.-C. Simulated annealing study of morphological transitions of diblock copolymers in solution. *J. Chem. Phys.* **2005**, *122*, 204905−8. (b) Kong, W.; Li, B.; Jin, Q.; Ding, D.; Shi, A.-C. Helical Vesicles, Segmented Semi vesicles, and Noncircular Bilayer Sheets from Solution-State Self-Assembly of ABC Miktoarm Star Terpolymers. *J. Am. Chem. Soc.* **2009**, *131*, 8503−8512.
(30) Metropolis, N.; Rosenbluth, A. W.; Rosenbluth, M. N.; Teller, A. H.; Teller, E. Equation of State Calculations by Fast Computing Machines. *J. Chem. Phys.* **1953**, *21*, 1087−1092.
(31) (a) Kubowicz, S.; Baussard, J.-F.; Lutz, J.-F.; Thünemann, A. F.; von Berlepsch, H.; Laschewsky, A. Multicompartment Micelles Formed by Self-Assembly of Linear ABC Triblock Copolymers in Aqueous Medium. *Angew. Chem., Int. Ed.* **2005**, *44*, 5262−5265. (b) Kubowicz, S.; Baussard, J.-F.; Lutz, J.-F.; Thünemann, A. F.; von Berlepsch, H.; Laschewsky, A. Multikompartiment-Micellen durch Selbstorganisation von linearen ABC-Triblock-Copolymeren in wässriger Lösung. *Angew. Chem., Int. Ed.* **2005**, *117*, 5397−5400. (c) Uchman, M.; Stepanek, M.; Prochazka, K.; Mountrichas, G.; Pispas, S.; Voets, I.-K.; Walther, A. Multicompartment Nanoparticles Formed by a Heparin-Mimicking Block Terpolymer in Aqueous Solutions. *Macromolecules* **2009**, *42*, 5605−5613. (d) Schacher, F.; Walther, A.; Ruppel, M.; Drechsler, M.; Müller, A. H. E. Multicompartment Core Micelles of Triblock Terpolymers in Organic Media. *Macromolecules* **2009**, *42*, 3540−3548. (e) Betthausen, E.; Drechsler, M.; Förtsch, M.; Schacher, F. H.; Müller, A. H. E. Dual stimuli-responsive multicompartment micelles from triblock terpolymers with tunable hydrophilicity. *Soft Matter* **2011**, *7*, 8880−8891.
(32) Zhang, J.; Lu, Z.; Sun, Z. A possible route to fabricate patchy nanoparticles via self-assembly of a multiblock copolymer chain in one step. *Soft Matter* **2011**, *7*, 9944−9950.
(33) Holmes, R. M.; Williams, D. R. M. Single Chain Asymmetric Block Copolymers in Poor Solvents. Candidates for Patchy Colloids. *Macromolecules* **2011**, *44*, 6172−6181.
(34) Jiang, T.; Wang, L.; Lin, S.; Lin, J.; Li, Y. Structural Evolution of Multicompartment Micelles Self-Assembled from Linear ABC Triblock Copolymer in Selective Solvents. *Langmuir* **2011**, *27*, 6440−6448.
(35) Ma, Z.; Yu, H.; Jiang, W. Bump-Surface Multicompartment Micelles from a Linear ABC Triblock Copolymer: A Combination Study by Experiment and Computer Simulation. *J. Phys. Chem. B* **2009**, *113*, 3333−3338.
(36) Dupont, J.; Liu, G. ABC triblock copolymer hamburger-like micelles, segmented cylinders, and Janus particles. *Soft Matter* **2010**, *6*, 3654−3661.
(37) Parsons, D. F.; Williams, D. R. M. Single Chains of Block Copolymers in Poor Solvents: Handshake, Spiral, and Lamellar

Globules Formed by Geometric Frustration. *Phys. Rev. Lett.* **2007**, *99*, 228302−4.
(38) Zhu, Y.; Yu, H.; Wang, Y.; Cui, J.; Kong, W.; Jiang, W. Multicompartment micellar aggregates of linear ABC amphiphiles in solvents selective for the C block: a Monte Carlo simulation. *Soft Matter* **2012**, *8*, 4695−4707.